J Membrane Biol (2010) 236:203–214
DOI 10.1007/s00232-010-9293-y

The Effect of Holding Potential on Charge Translocation by the Na^+/K^+-ATPase in the Absence of Potassium

Yanli Ding · Robert F. Rakowski

Received: 16 January 2010 / Accepted: 20 July 2010 / Published online: 10 August 2010

Abstract The Na^+/K^+-ATPase exports $3Na^+$ and imports $2K^+$ at the expense of the hydrolysis of 1 ATP. In the absence of K^+, it carries on electroneutral, Na^+-dependent transient charge movement (also known as "electroneutral Na^+/Na^+ exchange mode") and produces a transient current containing faster and slower components in response to a sudden voltage step. Components with different speeds represent sequential release of Na^+ ions from three binding sites. The effect of holding potential on slow charge movement was studied in the presence of different concentrations of ADP_i, Na_i^+ and Na_o^+ with the intention of improving our understanding of Na_i^+ binding. However, the manipulation of $[ADP]_i$ and $[Na^+]_i$ did not cause as pronounced changes as predicted in the magnitude of charge movement (Q_{tot}), which indicated that our experimental conditions were not able to backwardly drive reaction across the energy barrier to Na_i^+ release/rebinding steps. On the contrary, lowering $[Na^+]_o$ caused evident dependence of Q_{tot} on holding potential, with characteristics suggesting that pumps were escaping from E2P through the uncoupled Na^+ efflux activity.

Keywords Electrophysiology · Sodium pump · Voltage-clamp study · Biophysics

Introduction

The Na^+/K^+-ATPase (NKA), a member of the P-type ATPase protein family, is an integral membrane protein that exports $3Na^+$ and imports $2K^+$ at the expense of the hydrolysis of 1 ATP. The reaction catalyzed by NKA requires four substrates, intracellular Na^+ (Na_i^+), extracellular K^+ (K_o^+), ATP and H_2O, and produces four products, extracellular Na^+ (Na_o^+), intracellular K^+ (K_i^+), ADP and orthophosphate. NKA pumps ions in and out of the cell following a transport cycle usually referred to as the "Albers-Post scheme" (Fig. 1) (Albers 1967; Post et al. 1972; Skou and Esmann 1992). In this model, NKA can adopt two main conformations: E1 and E2. In E1, ion-binding sites face the cytoplasm and the apparent affinity for Na^+ is higher than that for K^+. In E2, ion-binding sites are exposed to the extracellular solution and the apparent affinity for K^+ is higher than that for Na^+. Phosphorylation of E1 by ATP promotes the occlusion (or trapping) of three intracellular Na^+, which are released to the external medium by a deocclusion transition associated with a conformational change to E2. Once two external K^+ bind to two of the three ion-binding sites, they elicit dephosphorylation and K^+ occlusion. ATP binding favors transition back to E1, prompting K^+ release to the cytoplasm and binding of three Na^+ ions to complete the cycle.

Under physiological conditions, NKA produces a net movement of one positive charge in the outward direction in each cycle. Consequently, the velocity at which the pump cycles (or turnover rate) must be sensitive to membrane potential (V_m). Most of the voltage dependence under normal ionic conditions comes from the transport of Na^+ (Rakowski 1993; Rakowski and Paxson 1988; Nakao and Gadsby 1986; Sagar and Rakowski 1994). Also, the major voltage-sensitive step occurs during Na_o^+ deocclusion/occlusion and release/binding steps (Rakowski et al. 1989, 1997). This can be explained by postulating the existence of a narrow and deep access channel or "ion well" between the Na^+-binding sites within the protein and the extracellular

Y. Ding (✉) · R. F. Rakowski
Department of Biological Sciences, Ohio University, Athens, OH 45701, USA
e-mail: yd364904@ohio.edu

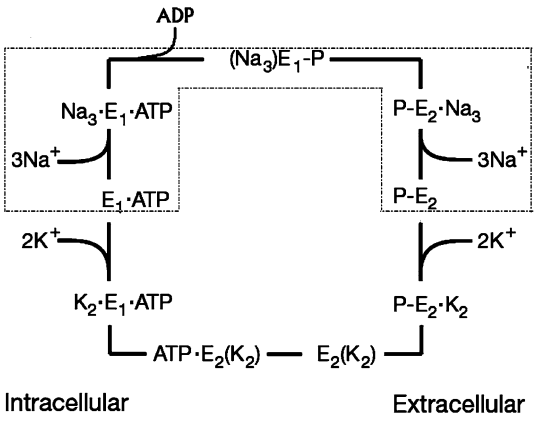

Fig. 1 Albers-Post scheme for the Na^+/K^+-ATPase

aqueous solution. Because the electric field is expected to drop along an access channel, negative potentials will favor binding of external Na^+ and, consequently, the forward pump turnover rate will be slowed down. The access channel model predicts that changes in ion concentration and membrane voltage are equivalent.

Removing K^+ from the experimental solutions restricts the pump to operating among the states encircled by dashed lines in Fig. 1. In this mode, NKA exchanges Na^+ with extracellular or intracellular medium without net movement of ions across the membrane or net hydrolysis of ATP.

At any given potential, the state occupancy of pumps is determined by the values of the rate constants. A sudden voltage step will instantly change any voltage-dependent rate constant, and the system will relax to the newly imposed steady state following a time course established by the new values of the rate constants (Nakao and Gadsby 1986). Therefore, depolarizing and hyperpolarizing steps elicited outward and inward transient currents, respectively. These currents decayed exponentially with time constants that were faster at hyperpolarizing voltages and reached a minimum at positive potentials. The voltage dependence of the charge (Q) follows a sigmoid shape, with saturations at large hyperpolarizing and depolarizing potential. These data could be well fitted by a Boltzmann distribution, as shown in Eq. 1 (see the Appendix for more explanation),

$$\frac{Q(V)-Q_{\min}}{Q_{\text{tot}}}=\frac{1}{1+\exp\left[\frac{zF(V_{\text{mid}}-V)}{RT}\right]} \quad (1)$$

where Q_{tot} is the total amount of charge, $Q_{\min}$ is the minimum value of charge reached at extreme negative voltages, V_{mid} is the mid-point voltage, F is Faraday's constant, R is the gas constant, T is temperature and z is apparent valence. z can be expressed as $n\lambda$, where n is the Hill coefficient representing the apparent molecularity of the charge moving process and λ is the dielectric coefficient representing the electric field dropped between external medium and the binding site. RT/zF represents the steepness of the curve.

With improvements of electrophysiological techniques in later studies, transient currents with fast relaxation rates were resolved. The exponential decay of the whole transient current was separated into three components, reflecting the deocclusion/release of three Na^+, which occurred in sequence with increasing rate constants from the first (1,000 s^{-1}), the second (about 6,000–20,000 s^{-1}) to the third (10^6 s^{-1}) Na^+ ions (Holmgren et al. 2000). The release or rebinding of the first Na^+ from E2P (Na3) or to E2P (Na2) forms the slow component and is the dominant charge-carrying step with a dielectric coefficient of 0.65–0.7 (Holmgren and Rakowski 2006; Holmgren et al. 2000; Wuddel and Apell 1995).

There are three other electrogenic partial reactions in the Post-Albers cycle: (1) the third intracellular Na^+ binding, $Na2 \cdot E1 \cdot ATP + Na_i^+ \rightarrow Na3 \cdot E1 \cdot ATP$ (Heyse et al. 1994; Wuddel and Apell 1995); (2) the conformational change, E1P(Na3) → E2P(Na3) (Heyse et al. 1994; Wuddel and Apell 1995); and (3) the extracellular K^+ binding, $E2P + 2K^+ \rightarrow E2 \cdot K2$ (Heyse et al. 1994; Sagar and Rakowski 1994; Wuddel and Apell 1995). Binding of the first two intracellular Na^+ ions was found to be electroneutral since it is accompanied by exchange for bound H^+ (Domaszewicz and Apell 1999). According to the conservation principle, the sum of all dielectric coefficients from each electrogenic partial reaction involved in transferring each net charge across the membrane has to be 1 (Apell 2003). The values presently determined for the dielectric coefficients are the third Na^+ binding to the intracellular binding site, 0.25 (Domaszewicz and Apell 1999); the conformational change, 0.1–0.2 (Heyse et al. 1994); the release of the first Na^+ to the extracellular medium, 0.65 (Hilgemann 1994; Holmgren et al. 2000); the release of the other two Na^+ to the extracellular medium, each 0.1 (Heyse et al. 1994; Hilgemann 1994); and the binding of two K^+ to their binding sites, each −0.1 to −0.2 (Heyse et al. 1994; Rakowski et al. 1991). The sum of these values is approximately 1, which obeys the conservation principle because the pump moves one net charge per cycle (Apell 2003).

The kinetics of the internal Na^+ binding and release step is the least-studied part of the transport cycle. This step has a rate that is not readily detected by current techniques, so it is impossible to study its kinetics directly. However, when this step is included in the reaction scheme, it can affect the availability of pumps for extracellular Na^+ release. We are trying to observe it indirectly through recording its effect on extracellular Na^+ release.

The slow charge translocation (Q_{slow}) that we measure comes from transitions involving extracellular Na^+ binding/unbinding and occlusion/deocclusion, which we could isolate fairly well by specifying the composition of the

internal and external solutions. If all pumps are confined to these states, we would expect no difference in the total amount of charge at different holding potential (V_h). We hypothesize that by manipulating $[ADP]_i$, $[Na^+]_i$ or $[Na^+]_o$, we will allow pumps to exit these states through a V_h-dependent route. After holding the membrane at a potential for enough time, the state occupancy is at an equilibrium determined by the rates of all participating steps, including internal Na^+-binding/release steps that are separated from external Na^+ release/rebinding by a very slow conformational change. Thus, by varying V_h and studying the corresponding change in Q_{slow}, we were expecting to infer the kinetics of internal Na^+ release/rebinding. If there is another V_h-dependent route, we would get to know the nature of the voltage dependence of that route.

At a constant V_h, changes in $[Na^+]_o$ and $[ADP]_i$ in previous studies did not affect the magnitude of the total mobile charge (Holmgren and Rakowski 2006), but V_{mid} was shifted toward more positive voltage by increasing $[Na^+]_o$ or $[ADP]_i$. A change of $[ADP]_i$ from 0 to 4.3 mM shifted V_{mid} 16 ± 6 mV (Peluffo 2004), and every doubling of $[Na^+]_o$ similarly shifted V_{mid} by ~20 to 25 mV (Holmgren and Rakowski 2006).

At a constant V_h, changes in $[Na^+]_i$ in previous studies did change the total amount of charge following a simple dose-response curve with an apparent affinity of 3.2 mM (Holmgren and Rakowski 2006). Because these data involve intracellular Na^+ binding and occlusion, the authors based their results on the following scheme:

$$3Na_i + E_iATP \overset{K_m(V_h)}{\leftrightarrow} (Na_3)E_1P \cdot ADP \underset{K_{-1}}{\overset{k_1}{\rightleftharpoons}} (Na_3)E_1P \underset{K_{-2}}{\overset{k_2}{\rightleftharpoons}} E_2P + 3Na_o \quad \text{(Scheme 1)}$$

Therefore, charge (Q) becomes a function of voltage and $[Na^+]_i$ by

$$Q(V) = \left[\frac{Q_{tot}}{1+\exp\left(\frac{zF(V_{mid}-V)}{RT}\right)} + Q_{min}\right]\left[\frac{[Na]_i}{[Na]_i + K_m(V_h)}\right] \quad (2)$$

where $K_m(V_h)$ is a voltage-dependent dissociation coefficient for binding of the third intracellular Na^+. Therefore, estimating Q_{tot} at different V_h but constant $[Na^+]_i$, we expected to learn about the intrinsic voltage dependence of intracellular Na^+ binding.

Materials and Methods

Oocyte Preparation and Maintenance

The charge movement (Q) mediated by Na^+ release and rebinding was measured using the cut-open oocyte voltage-clamp technique in *Xenopus laevis* oocytes expressing *Bufo marinus* NKA α_1- and β_1-subunits. Oocytes at stages V and VI were collected and treated with 0.3% collagenase in Ca^{2+}-free ND96 solution (96 mM NaCl, 2 mM KCl, 1 mM $MgCl_2$, 2.5 mM Na pyruvate, 5 mM Tris HEPES [pH 7.3], osmolarity = 200 ± 5) for 40–60 min to remove the follicular layer. Oocytes remained viable for up to 6 days at 15°C in ND96 solution (Ca^{2+}-free ND96 plus 1.8 mM $CaCl_2$).

RNA Preparation and Injection

Wild-type *B. marinus* NKA α_1 and β_1 cRNAs were transcribed from their corresponding cDNAs. *B. marinus* NKA α_1 and β_1 cDNAs in plasmid pSD5 were transformed into competent bacteria DH5α, single colonies were grown overnight and plasmids were prepared using the QIAprep Spin Miniprep Kit 27104 (Qiagen, Valencia, CA).

The extracted α_1 and β_1 cDNAs were linearized by restriction enzymes *Spe*I and *Bgl*II (New England Biolabs, Ipswich, MA), respectively. Linearized cDNAs were treated with proteinase K and extracted using phenol/chloroform. cRNAs were transcribed from linearized cDNAs using the MAXIscript® SP6 Kit (AM1308; Ambion, Austin, TX). Ten nanograms of α_1 cRNA and 1 ng of β_1 cRNA were coinjected into oocytes 1 day after oocytes were collected. Injected oocytes were incubated in ND96 solution for 3 days to obtain good membrane expression. Oocytes were incubated overnight in 0.2 μM ouabain containing ND96 solution to inhibit the endogenous *X. laevis* NKA current (Horisberger and Kharoubi-Hess 2002). *B. marinus* α_1 is more ouabain-resistant than *X. laevis* α_1 so that pretreatment in 0.2 μM ouabain completely inhibits the endogenous pump current but has little effect on the introduced *Bufo* pump current, while the 1 mM ouabain applied during electrophysiological measurement inhibits both kinds of current.

Cut-Open Setup and Recording Protocols

Saponin-permeabilized *Xenopus* oocytes mounted with guarded seals between the intracellular and extracellular compartments were used to study transient currents mediated by *Bufo* NKA (Taglialatela et al. 1992). Compared to a regular two-microelectrode voltage-clamp recording of whole-oocyte currents, this setup has several advantages, including (1) high-frequency response and low noise recording, (2) access to the cell interior and (3) stable recording conditions lasting for several hours.

The oocyte was mounted with its animal (dark) pole oriented toward the bottom, where it was permeabilized by adding 0.5% saponin for approximately 1 min. Permeabilization resulted in a decrease in access resistance and a large increase in linear nonpump capacitance, which resulted in an

increase in the time constant of total transient currents induced by small-amplitude (20 mV) test voltage-clamp pulses (stepping from 0 to −20 mV). Then, the saponin solution was replaced by the experimental intracellular solution and allowed to equilibrate until there was no change in transient current magnitude. Oocytes were stable with small background current for more than 2 h. The voltage-clamp system was obtained from Dagan (Minneapolis, MN; model CA-1 High Performance Oocyte Clamp).

The effects of three different V_h (−20, −60 and −100 mV) were studied in permeabilized oocytes as $[Na^+]_i$, $[ADP]_i$ and $[Na^+]_o$ were varied. Voltage pulses of 40 ms duration were made from V_h to command potentials over the range −160 to +60 mV in increments of 20 mV. Pulses were applied every 300 ms, and the current records were obtained by averaging four repetitions of the pulse protocol. Three V_h were applied in the order of −60, −100 and −20 mV. To study the effect of V_h in low $[Na^+]_o$ in detail, six V_h were applied in the order of −40, −80, 0, −60, −100 and −20 mV. The time elapsed before and after the addition of ouabain at each V_h was the same. Two V_h of −20 mV were applied to bracket the entire series of V_h both before and after the addition of ouabain (Fig. 2). The current differences between the bracketing V_h of −20 mV were checked to make sure that only small time-dependent drifting happened.

Data were acquired using an analog-to-digital converter system and software (TL-1 DMA interface, 100 kHz, PCLAMP version 9; Molecular Devices, Sunnyvale, CA) running on a Dell-compatible computer system (Austin, TX). The analog signal was filtered at 5 kHz before being digitized and sampled every 20 μs.

Solutions

The 100 Na0 K external solution had the following composition: 100 mM Na glutamate, 20 mM tetraethylammonium (TEA) glutamate, 3 mM Mg $(glutamate)_2$, 5 mM $Ba(NO_3)_2$, 2 mM $Ni(NO_3)_2$, 0.01 mM $Gd(NO_3)_3$, 0.3 mM niflumic acid and 10 mM Tris HEPES (pH 7.6). 25 Na0 K external solution was obtained by equimolar substitution of tetramethylammonium (TMA) for Na^+. The composition of 50 Na0 K internal solution was 50 mM Na glutamate, 20 mM TEA glutamate, 10 mM $MgSO_4$, 5 mM MgATP, 5 mM Tris ADP, 5 mM 1,2-bis(2-aminophenoxy)ethane-*N,N,N′,N′*-tetraacetic acid (BAPTA), 30 mM *N*-methyl D-glucamine (NMDG) glutamate, 10 mM 3-(*N*-morpholino)propanesulfonic acid (MOPS, pH 7.3). Na^+-free internal solution was prepared by equimolar substitution of NMDG for Na^+. Intermediate intracellular Na^+ concentrations were obtained by mixing internal solutions containing 50 and 0 mM Na_i^+. Note that both ATP and ADP were present in the intracellular solution, to promote electroneutral Na^+/Na^+ exchange (De Weer 1970; Glynn and Hoffman 1971). One millimolar P1,P5-di(adenosine-5′)pentaphosphate (AP5A) was included in all ADP-containing internal solutions, to prevent phosphate exchange between ATP and ADP. To study the ADP sensitivity of Q_{slow}, 5 mM phosphocreatine substituted 5 mM ADP to make sure no ADP was formed from ATP hydrolysis. The solutions were designed to minimize nonpump-mediated current. Extracellular TEA^+ and Ba^{2+} were present to block passive K^+ conductance (Holmgren and Rakowski 1994). NMDG was used as an internal Na^+ substitute

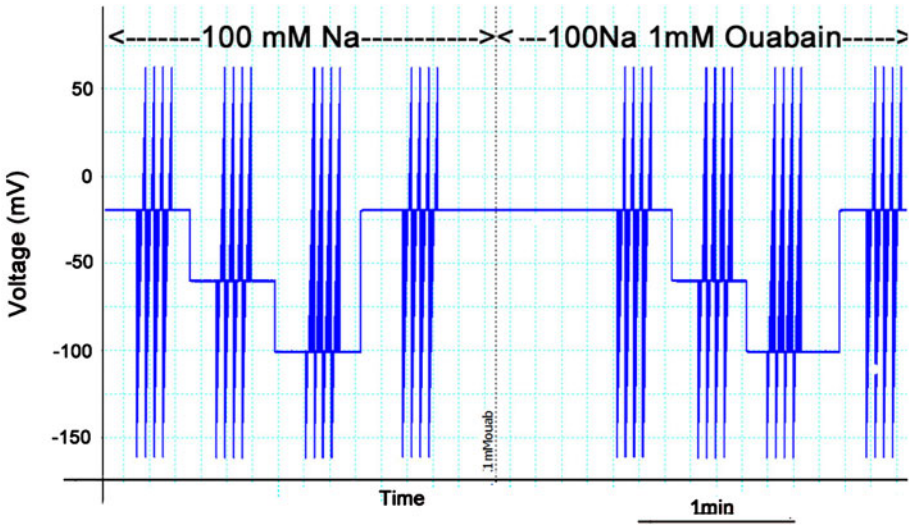

Fig. 2 Chart recording of holding potentials and voltage steps applied during a typical experiment. Oocyte was holding at −20, −60, −100, −20 mV in 100 or 25 mM Na_o^+ solution first. After equilibrating at each V_h for ~10 s, four runs of voltage steps ranging from −160 to 60 mV with increments of 20 mV were applied. Then, 1 mM ouabain was added to the external solution. After pumps were fully inhibited, the exact same sequence of voltage changes was applied. The time elapsed from before to after the addition of ouabain at each V_h was the same

because it would be less likely to compete for Na^+-binding sites than smaller cations. The solutions were nominally chloride-free and Ca^{2+}-free, to prevent activation of Ca^{2+}-dependent anionic current. Niflumic acid was present to block Cl^- channels. Ni^{2+} and Gd^{3+} were present to block Na^+/Ca^{2+} exchange (Kimura et al. 1987) and stretch-activated cation channels (Yang and Sachs 1989), respectively.

Transient Current Analysis

Na^+-dependent transient current was calculated by subtraction of the current records obtained after arresting Na^+-dependent charge movement by the addition of 1 mM ouabain from records acquired just prior to the addition of ouabain (Fig. 3). Previous studies have demonstrated that the slow ouabain-sensitive transient current is preceded by at least one fast component with a time course close to that of the voltage step (relaxation rate >2,000 s^{-1}) (Hilgemann 1994; Holmgren and Rakowski 2006; Holmgren et al. 2000). Therefore, to obtain the relaxation rate of slow components, transient currents were fitted with a single exponential function starting 2–4 ms after the initiation of voltage steps over a 30-ms period and the fit was extended to about 0.5 ms after the start of voltage steps to include the complete slow component without contamination by faster components. In another study of Na^+-dependent transient current, the fit was started about 0.5 ms after the beginning of the pulse (Colina et al. 2007); but in our study with *Bufo* NKA expressed in *Xenopus*, to get a good fit, the single exponential fit had to be started 2–4 ms after the beginning of the pulse (Fig. 4b, d). If the fit was started 0.5 ms after the beginning of the pulses, an exponential function with two components was needed for a good fit (Fig. 4c). This might be due to the difference in the NKAs between species. In order to observe the Na_o^+-dependent slow charge movement in full scale, the fit in our study was then extended to the beginning of the pulse (Fig. 4d).

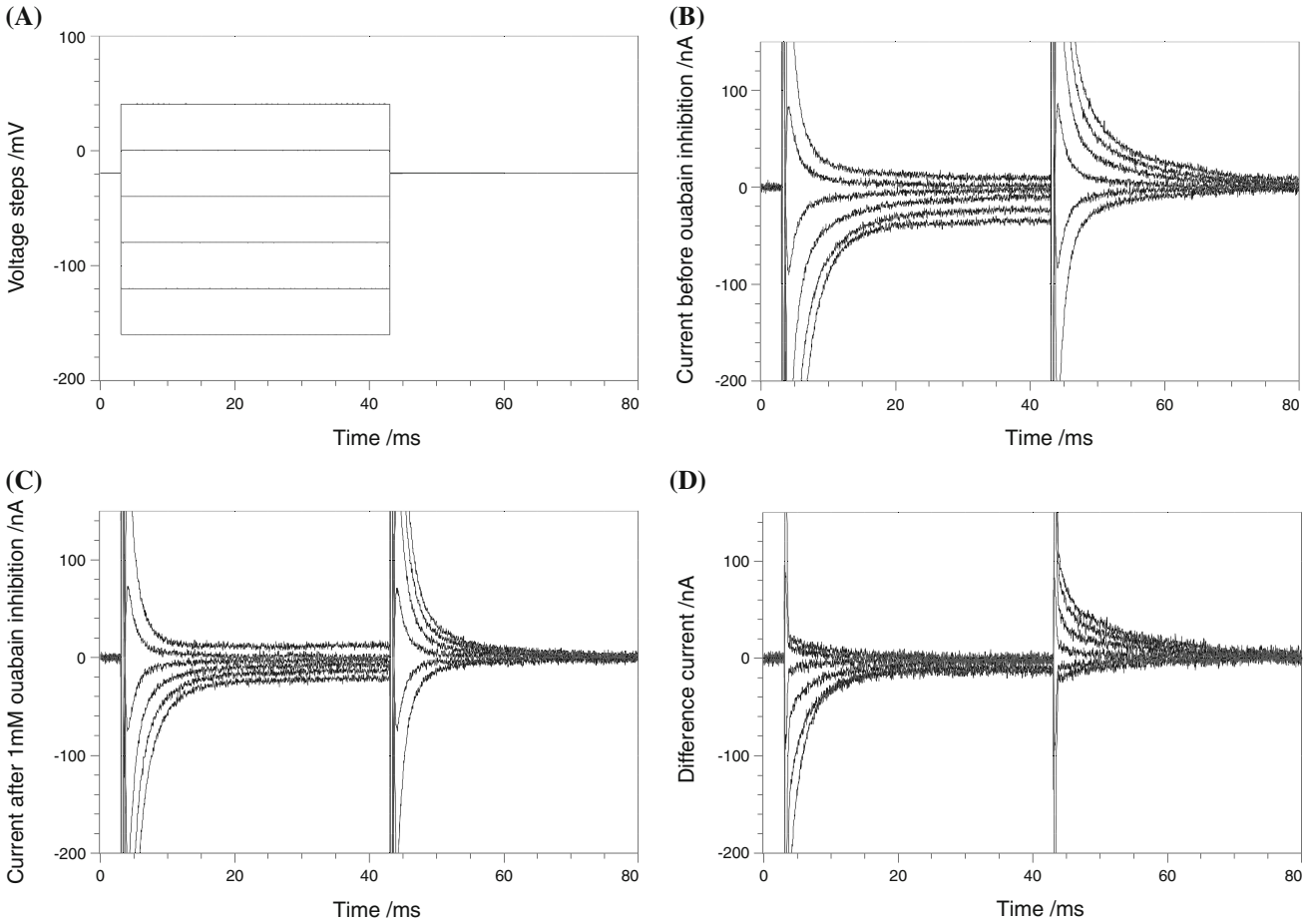

Fig. 3 Ouabain-sensitive transient currents from a permeabilized oocyte. **a** Voltage pulse protocol. Voltage pulses were done in increments of 20 mV from −160 to +60 mV with duration 40 ms. For clarity, voltage pulses are shown every 40 mV. Holding potential was −20. **b** Current time course in 100 Na0 K external solution. **c** Currents in 1 mM ouabain 100 Na0 K external solution. **d** Ouabain-sensitive currents determined by subtraction of currents in the presence of 1 mM ouabain (**c**) from those in its absence (**b**)

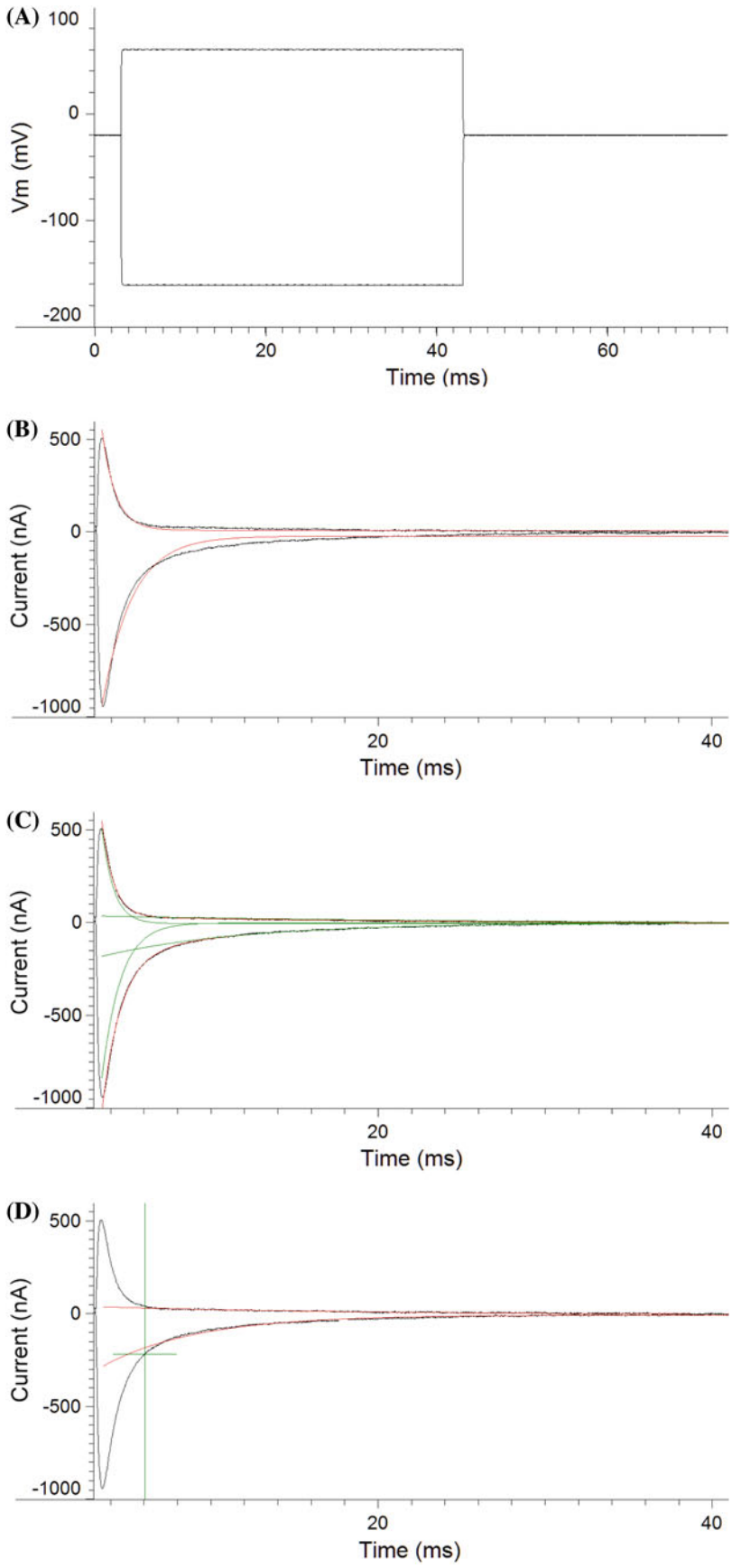

Fig. 4 Different fitting methods applied to the subtracted currents obtained from an oocyte in 25 mM Na_o^+ and 10 mM Na_i^+. **a** Voltage steps used to elicit currents. For simplicity, two voltages, 60 and −160 mV, are shown. The 60-mV step elicited an outward transient current and −160 mV elicited an inward transient current, shown in (**b–d**), where the same currents (*dark lines*) were fitted differently. **b** The subtracted currents were fitted starting 0.5 ms after the beginning of pulses with a single-exponential function. *Red lines* (*light lines* in gray scale) represent the best fit. **c** The subtracted currents were fitted starting 0.5 ms after the beginning of pulses with a two-component exponential function. *Red lines* (overlapping raw data) represent the best fit. *Green lines* (*light lines* in gray scale) represent fitted components. **d** The subtracted currents were fitted starting 3 ms after the beginning of pulses with a single-exponential function. Meanwhile, fit was extended to the beginning of pulses. *Vertical line* represents the time point when fit started. *Red lines* (*light lines* in gray scale) represent the best fit (Color figure online)

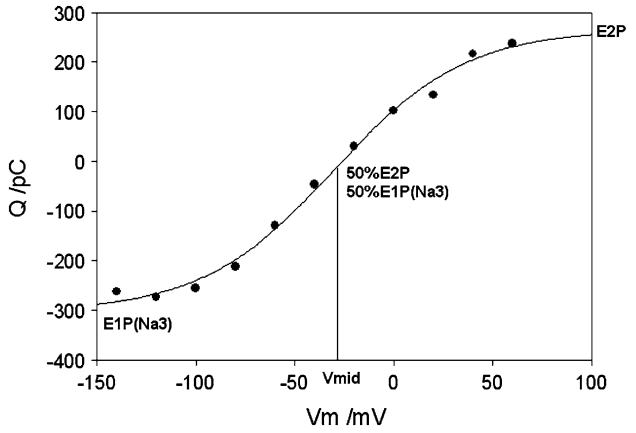

Fig. 5 An example of voltage (V_m) dependence of charge distribution (Q) (Q–V curve). *Solid line* represents the best-fit line of the data points using Eq. 1. Q_{max} at extreme positive V_m represents when 100% of the measured pumps are in state E2P (no Na^+ bound), and Q_{min} at extreme negative V_m represents when 100% are in state E1P(Na_3) ($3Na^+$ bound). V_{mid} represents when half of the pumps are in state E2P and half in E1P(Na_3)

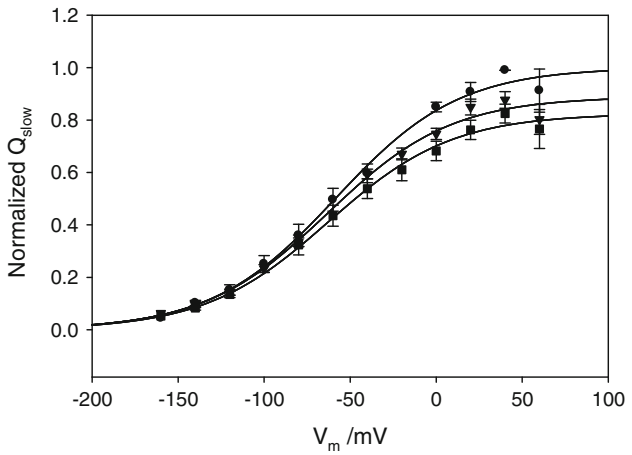

Fig. 6 The V_h dependence of the Q–V curve of ouabain-sensitive transient currents in oocytes in internal solution 50 mM Na^+, 5 mM ATP, 0 ADP and 0 K^+ and externally perfused with 100 mM Na^+0 K^+. Dots are data points (mean ± SE) at V_h of −20 mV (*circles*), −60 mV (*triangles*) and −100 mV (*squares*). *Solid lines* represent best fit to Eq. 1 with z constrained to 0.71. The z value was obtained by initially fitting the Q–V curve at V_h −20 mV to Eq. 1 with z floating. The best-fit parameter values are $Q_{tot} = 1.00 \pm 0.03$, $V_{mid} = -58.7 \pm 5.3$ mV for $V_h = -20$ mV; $Q_{tot} = 0.89 \pm 0.02$, $V_{mid} = -63.1 \pm 4.8$ mV for $V_h = -60$ mV; $Q_{tot} = 0.82 \pm 0.03$, $V_{mid} = -62.6 \pm 6.4$ mV for $V_h = -100$ mV. Data were from five oocytes of at least two different frogs

Q_{slow} was then determined by multiplying the two parameters A (the fitted initial value of transient currents) and tau (time constant of exponential decay of transient currents), obtained by the single exponential fit. All of this analysis was done with Clampfit 9.2 software. Further analysis, least-squares curve fitting and preparation of figures were done with SigmaPlot 8.0 (Systat Software, Richmond, CA). Curve-fit parameters were obtained from the least-squares fitting procedure. Experiments were performed at room temperature (~22°C).

The voltage dependence of the charge movement (Q–V curve) is given by Eq. 1, which has a sigmoid shape. To simplify the meaning of the curve, Q_{max} represents the maximum occupation of pumps at Na^+-free form E2P and Q_{min} represents the maximum occupation of pumps at Na^+-binding form E1P(Na3) (Fig. 5).

Results

Equation 1 was used to fit Q–V curves obtained under different conditions. The value of V_{mid}, representing the position of the curve, depends on the ratio between the occupancies of E1P(Na3) and E2P states at a certain voltage. V_{mid} is always the voltage where the ratio is 1 (Fig. 3). The z value is the apparent valence of the charge moved between those states, which floats at V_h of −20 mV and then is constrained to the value obtained at V_h of −20 mV for all Q–V curves under the same intracellular and extracellular conditions.

Effect of V_h on the Magnitude of Q_{slow} in 100 mM Na_o^+ and 50 mM Na_i^+ with or without 5 mM ADP

In the absence of ADP, Scheme 1 is reduced to

$$E1P(Na3) \leftrightarrow E2P + 3Na^+ \qquad \text{(Scheme 2)}$$

which includes the transitions eliciting the charge translocation that we measure (see the Appendix for more explanation). Therefore, we might expect that adding intracellular ADP should result in a reduction of the amount of charge.

Figure 6 shows how charge distributes (Q–V curve) at three different values of V_h, −20 (circle), −60 (triangle) and −100 mV (squares), and in the absence of ADP. All data from each oocyte were normalized to the Q_{tot} obtained at V_h of −20 mV. Then, data from five oocytes of at least two frogs were pooled together and fitted again to obtain the best-fit parameters Q_{tot}, V_{mid} and z. Q_{tot} showed slight dependence on V_h. Q_{tot} was 0.88 ± 0.02 at V_h of −60 mV and 0.82 ± 0.03 at V_h of −100 mV.

Figure 7 shows the charge distribution from a similar set of experiments but in the presence of 5 mM intracellular ADP. Clearly, under the present experimental conditions, ADP has no effect on the amount of charge moved at different V_h, suggesting that ADP could not displace pumps toward the intracellular Na^+-binding/release transitions. This failure could be because there was not enough

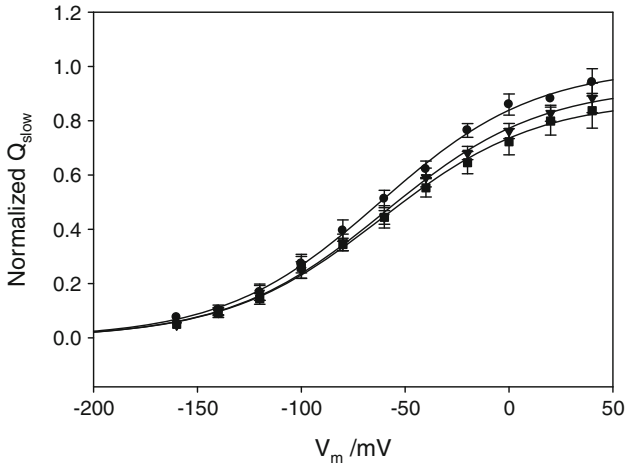

Fig. 7 The V_h dependence of the Q–V curve of ouabain-sensitive transient currents in oocytes in internal solution 50 mM Na^+, 5 mM ATP, 5 mM ADP and 0 K^+ and externally perfused with 100 mM Na^+0 K^+. Dots are data points (mean ± SE) at V_h of −20 mV (*circles*), −60 mV (*triangles*) and −100 mV (*squares*). *Solid lines* represent best fit to Eq. 1 with z constrained to 0.68. The z value was obtained by initially fitting the Q–V curve at V_h −20 mV to Eq. 1 with z floating. The best-fit parameter values are $Q_{tot} = 1.00 \pm 0.03$, $V_{mid} = -62.2 \pm 4.8$ mV for $V_h = -20$ mV; $Q_{tot} = 0.93 \pm 0.03$, $V_{mid} = -59.8 \pm 5.3$ mV for $V_h = -60$ mV; $Q_{tot} = 0.88 \pm 0.03$, $V_{mid} = -61.5 \pm 6.7$ mV for $V_h = -100$ mV. Data were from five oocytes from at least two different frogs

difference between intracellular and extracellular [Na^+] to drive the pumps backward.

Effect of V_h on the Magnitude of Q_{slow} in 100 mM Na_o^+ and 10 mM Na_i^+ or 1 mM Na_i^+

In an attempt to increase the transmembrane difference in [Na^+], we performed similar experiments in the presence of 5 mM ADP and 100 mM $[Na^+]_o$ but decreased the intracellular [Na^+] from 50 to 10 or 1 mM. Previously, it was shown that $K_m(0)$ for intracellular Na^+ binding is 3.2 mM for endogenous *Xenopus* NKA (Holmgren and Rakowski 2006). Assuming that *Bufo* NKA $\alpha_1\beta_1$ has a similar apparent affinity, then the changes of $[Na^+]_i$ in our study would cover a large range of the dose-response curve.

Figure 8 shows that in the presence of 10 mM or 1 mM Na_i^+ Q_{tot} does not change with different holding potentials, suggesting that not even a 100-fold difference between intracellular and extracellular [Na^+] was enough to drive the pumps toward the inward-facing Na^+-binding sites.

Effect of V_h on the Magnitude of Q_{slow} at Low $[Na^+]_o$

Figure 9a shows Q–V curves in the presence of 25 mM Na_o^+ obtained at different V_h. The other conditions in this set of data were 10 mM Na_i^+, 5 mM ADP and 5 mM ATP.

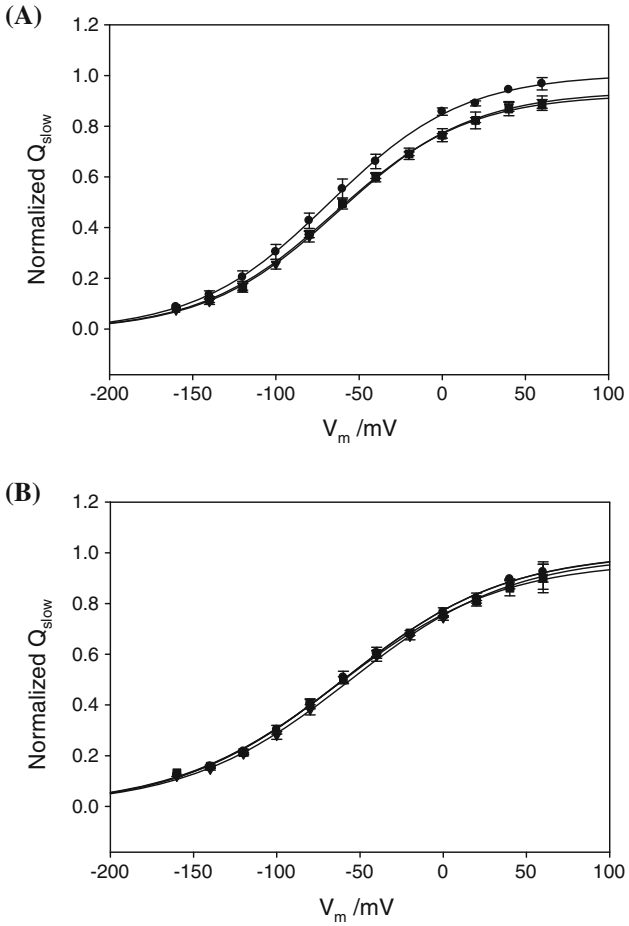

Fig. 8 The V_h dependence of the Q–V curve of ouabain-sensitive transient currents in 10 and 1 mM Na_i^+. Oocytes were incubated in internal solution (in mM: 5 ADP, 5 ATP and 0 K^+) and externally perfused with 100 Na^+0 K^+. **a** The voltage dependence of normalized charge (Q_{slow}) in 10 mM at V_h of −20 mV (*circles*), −60 mV (*triangles*) and −100 mV (*squares*). Dots are data points (mean ± SE). *Solid lines* represent the best fit to Eq. 1 with z constrained to 0.63. The z value was obtained by initially fitting the Q–V curve at V_h −20 mV to Eq. 1 with z floating. The best-fit parameters are $Q_{tot} = 1.00 \pm 0.02$, $V_{mid} = -67.9 \pm 3.7$ for $V_h = -20$ mV; $Q_{tot} = 0.95 \pm 0.01$, $V_{mid} = -62.4 \pm 2.9$ for $V_h = -60$ mV; $Q_{tot} = 0.93 \pm 0.02$, $V_{mid} = -64.7 \pm 3.7$ for $V_h = -100$ mV. **b** The voltage dependence Q_{slow} in 1 mM. Symbols are the same as in **a**. The z value is 0.52, which was obtained by initially fitting the Q–V curve at V_h −20 mV to Eq. 1. The best-fit parameter values are $Q_{tot} = 1.00 \pm 0.02$, $V_{mid} = -60.1 \pm 4.7$ for $V_h = -20$ mV; $Q_{tot} = 0.99 \pm 0.02$, $V_{mid} = -56.5 \pm 5.0$ for $V_h = -60$ mV; $Q_{tot} = 0.97 \pm 0.02$, $V_{mid} = -63.0 \pm 5.4$ for $V_h = -100$ mV. Data were from five or six oocytes of at least two frogs

Interestingly, the more negative V_h was, the less Q_{tot} we could estimate, as if holding at negative potential effectively removed pumps from the states shown in Scheme 2. In fact, Q_{tot} appeared to follow a sigmoid distribution with V_h (Fig. 9b). If we assume that our system is losing pumps through a single voltage-dependent transition, then it would be rather strong voltage dependence with an apparent valence of 2.6.

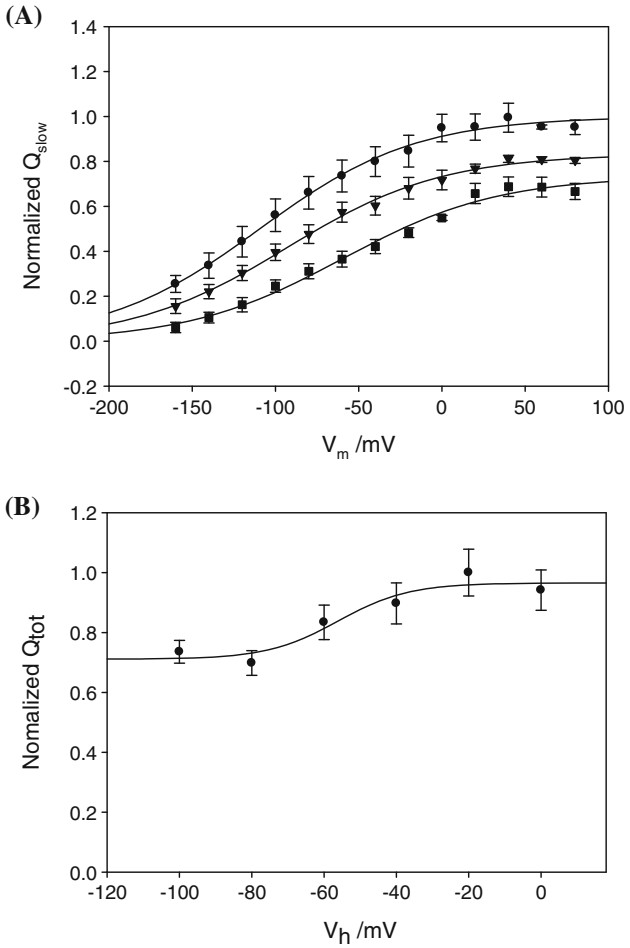

Fig. 9 Effect of holding potential on ouabain-sensitive transient current in oocytes in internal solution 10 mM Na^+, 5 mM ADP, 5 mM ATP and 0 K^+ and externally perfused with 25 mM Na_o^+. **a** Voltage dependence of Q_{slow} at V_h of −20 mV (*circles*), −60 mV (*triangles*) and −100 mV (*squares*). Dots are data points (mean ± SE). *Solid lines* represent the best fit to Eq. 1 with $z = 0.54$. The z value was obtained by initially fitting the Q_{slow} vs. V_m curve at V_h −20 mV to Eq. 1 with z floating. The best-fit parameter values are $Q_{tot} = 1.00 \pm 0.07$, $V_{mid} = -109.0 \pm 15.8$ mV for $V_h = -20$ mV; $Q_{tot} = 0.83 \pm 0.05$, $V_{mid} = -93.0 \pm 9.6$ mV for $V_h = -60$ mV; $Q_{tot} = 0.73 \pm 0.03$, $V_{mid} = -59.8.8 \pm 8.6$ mV for $V_h = -100$ mV. **b** V_h dependence of Q_{tot}. Values of Q_{tot} were obtained by fitting Q–V curves at six V_h, 0, −20, −40, −60, −80 and −100 mV, to Eq. 1 with $z = 0.54$ and then normalizing to the value obtained at V_h −20 mV. Dots are data points (mean ± SE). *Solid line* is the best fit to the Boltzmann function. The best-fit z value is 2.6. Data were from four oocytes of two frogs

Discussion

E1P(Na3)/E2P Occupancy Under Different Conditions

To interpret the results, we have to once again review the rationale behind transient currents. There exists a dynamic equilibrium between the intermediate states in electroneutral Na^+/Na^+ exchange mode, which can be expressed in a more detailed form of Scheme 3 (see the Appendix for more explanation) (Wuddel and Apell 1995).

$$\begin{aligned} E1 \cdot ATP + 3Na &\leftrightarrow E1 \cdot ATP \cdot 3Na \\ &\leftrightarrow E1P(Na_3) \cdot ADP \leftrightarrow E1P(Na_3) \\ &\leftrightarrow E2P \cdot 3Na \leftrightarrow E2P \cdot 2Na \\ &\leftrightarrow E2P \cdot Na \leftrightarrow E2P \end{aligned} \quad \text{(Scheme 3)}$$

The distribution of pumps between these states depends on the concentration of substrates and products and on the membrane potential. In this study, we varied the concentrations of [ADP], $[Na^+]_i$ and $[Na^+]_o$ and the holding potential, V_h.

The charge translocation that we measured derives from a subset of transitions of Scheme 3, which relate to extracellular Na^+ binding/unbinding and occlusion/deocclusion—$E1P(Na_3) \leftrightarrow E2P \cdot 3Na \leftrightarrow E2P \cdot 2Na \leftrightarrow E2P \cdot Na \leftrightarrow E2P$. Within these transitions, negative potentials will displace the system toward the E1P(3Na), whereas positive potentials will shift the pumps toward the E2P state. If any experimental condition allows pumps to exit from this subset of charge translocation transitions, then we would expect a change in Q_{tot}. If the escape route is a voltage-dependent process, then the changes in Q_{tot} will be different depending on V_h, and these differences will provide information on the voltage-dependent steps that do not relate to the extracellular Na^+-binding/release transitions.

Effect of V_h on the Magnitude of Q_{slow} with 100 mM Na_o^+, 50 mM Na_i^+ in the Presence and Absence of ADP

In the presence of ADP, it is expected that pumps in the $E1P(Na_3)$ could, in principle, transit to $E1P(Na_3) \cdot ADP$ and then deocclude and release $3Na^+$ to the intracellular medium with the production of ATP. However, our results in Fig. 6 show that the presence of 5 mM ADP in the intracellular solution did not elicit significant change of Q_{tot} as V_h became more negative, similar to the results obtained in the absence of ADP (Fig. 6). Therefore, under both conditions, 50 mM Na_i^+ and/or 5 mM ATP was able to keep pumps from exiting the subset of charge translocation transitions.

Effect of V_h on the Magnitude of Q_{slow} with 5 mM ADP and Varying Na^+ Present Intracellularly

According to Eq. 2, we were expecting that changing V_h would affect the $Q(V)$ by a factor of $[Na]_i/([Na]_i + K_m[V_h])$, where K_m and V_h are related by

$$K_m(V_h) = K_m(0)\exp(-\lambda_i F V_h / RT) \quad (3)$$

where $K_m(0)$ is the apparent affinity for intracellular Na^+ and λ_i is the dielectric coefficient of intracellular Na^+

binding. We studied the effect of V_h on the pump-mediated charge translocation at three different $[Na^+]_i$ (1, 10 and 50 mM). Of all conditions in our study, low $[Na^+]_i$ was the condition that most favored pumps displacing toward the intracellular Na^+-binding steps. However, V_h has only minor changes in Q_{tot} in low $[Na^+]_i$ (Figs. 7 and 8), indicating that we were not able to displace pumps toward the intracellular Na^+-binding steps. The most feasible explanation is that the magnitude of the forward rate is difficult to overcome by changes in occupancy of the E1(3Na)-P state with voltage, once the intracellular ATP is 5 mM.

Effect of V_h on the Magnitude of Q_{slow} in 25 mM Na_o^+

By reducing extracellular Na^+ to 25 mM, we observed an unexpected result. At low Na_o^+, Q_{tot} follows a sigmoidal shape with V_h, suggesting that negative V_h somehow remove pumps from the subset of charge translocation transitions. Furthermore, the route by which these pumps escape is a strong voltage-dependent transition.

What route is being followed by the pumps? In the absence of K^+, it has been reported since the 1960s (Garrahan and Glynn 1967) that pumps could operate in several modes. The most favorable is the traditional Na^+/Na^+ electroneutral exchange, but under certain conditions the pump could transport either $3Na^+/2Na^+$, sometimes called Na^+ ATPase activity (Fig. 10a), or $3Na^+$ outwardly by an uncoupled ATPase activity (Fig. 10b) (Glynn and Karlish 1976; Heyse et al. 1994; Peluffo et al. 2000; Wuddel and Apell 1995).

Both transports are expected to be very slow processes. Therefore, experimental estimations of their reaction rate have been difficult. However, they have been estimated by numerical simulation utilizing other available values of the reaction cycle, and they are in the 10^{-1} s^{-1} range (Heyse et al. 1994). In principle, both of these noncanonical transport processes could provide escape routes for E2P. However, there are two reasons that suggest that uncoupled ATPase activity is the main source for escape. First, it has been previously documented that uncoupled ATPase activity is favored in low $[Na^+]_o$, contrary to the $3Na^+/2Na^+$ ATPase activity, which is enhanced by high $[Na^+]_o$ (Glynn and Karlish 1976; Heyse et al. 1994). In 50 mM Na_i^+, hyperpolarizing V_h causes a slight decrease in Q_{tot} in 100 mM Na_o^+ (Fig. 7). This effect of V_h becomes more pronounced when $[Na^+]_o$ decreases to 25 mM Na_o^+ (Fig. 9). Second, our observation that the escape route is strongly voltage-dependent is consistent with previous theoretical estimations of the voltage dependence of uncoupled ATPase activity. According to the conservation principle, the sum of the dielectric coefficients of steps involved in uncoupled ATPase activity has to be 3 because three net charges are transported across the membrane in each cycle

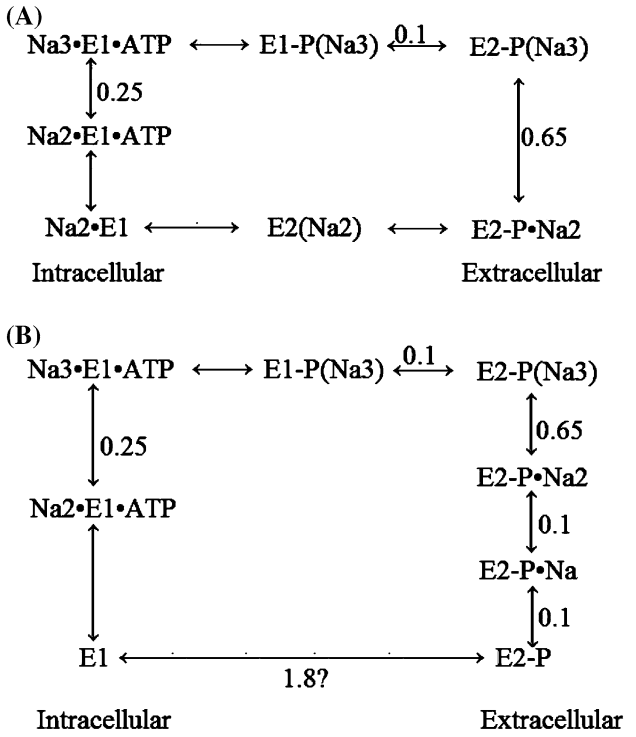

Fig. 10 Two possible operating modes of NKA other than electroneutral Na^+/Na^+ exchange in the absence of K^+. **a** The $3Na^+/2Na^+$ transport mode; **b** uncoupled ATPase activity with $3Na^+$ efflux and no cation influx. *Numbers beside lines* indicate the dielectric coefficients that the particular partial reactions go through. *Question mark* indicates that the value was estimated by previous theoretical estimations (Heyse et al. 1994) and has not been verified by experiments

(Apell 2003). Of all partial steps in this cycle, only the dielectric coefficient of transition from E2-P to E1 was not acquired experimentally but estimated based on these known values and the conservation principle (Heyse et al. 1994).

The slow spontaneous transition from E2-P to E1 with a rate of about 8×10^{-1} s^{-1} limits the turnover rate of uncoupled ATPase activity. The turnover rate of usual Na^+/K^+ transportation is 20–100 s^{-1} (Boardman et al. 1972), which means that we could observe a steady-state current in the absence of K^+ with about 1/100 magnitude compared to the K^+-activated pump current. The small magnitude of this current makes it very hard to record (Glynn and Karlish 1976). Future studies of the steady-state current mediated by the NKAs highly expressed in oocytes under low $[Na^+]_o$ and K^+-free conditions will provide more information on the kinetics of uncoupled Na^+ efflux.

Lack of an Effect of Varying [ADP] on Voltage Dependence of Slow Charge Movement

When Q–V curves in 50 mM Na_i^+, 5 mM ADP (Fig. 5) were compared to the curves recorded at the same V_h in 50 mM Na_i^+, 0 ADP (Fig. 4), we failed to observe any difference at

V_{mid}. For instance, at V_h of −20 mV, V_{mid} is −62.2 ± 4.8 mV (mean and SE) in the presence of 5 mM ADP and −58.7 ± 5.3 mV in the absence of ADP. However, Peluffo (2004) recorded that increasing [ADP] caused the Q–V curve to shift to more positive V_m, which indicates that the presence of ADP in rat cardiac myocytes facilitated the backward reaction in Na^+ translocation at half-cycle. A possible reason for this discrepancy is that the internal condition of 50 mM Na^+, 5 mM ADP and 5 mM ATP could not displace *Bufo marinus* NKA toward the intracellular Na^+-binding/release transitions, thus masking the subtle effect of [ADP] on the Na_o^+-dependent slow charge movement.

In summary, we studied the effect of V_h on Na_o^+-dependent slow charge movement mediated by *B. marinus* NKA expressed in *X. laevis* oocytes in different $[Na^+]_i$, [ADP] or $[Na^+]_o$. Lowering $[Na^+]_i$ and increasing [ADP] were expected to influence the Na_o^+-dependent slow charge movement by displacing pumps toward the intracellular Na^+-binding steps. However, these variations did not show the effect of V_h on slow charge movement. The possible explanation is that these conditions were not strong enough to push *Bufo* NKA backward to release Na^+ from $E1P(Na_3)$·ADP to the internal medium when 5 mM ATP was present internally. However, unexpectedly, lowering $[Na^+]_o$ brought out the inhibiting effect of hyperpolarizing V_h on slow charge movement. The strong V_h dependence of Q_{tot} in 25 mM Na_o^+ suggests uncoupled Na^+ efflux as a possible escape route of E2P in the absence of K^+.

Acknowledgement This article is dedicated to Dr. R. F. Rakowski. His earnest attitude to teaching and research and his open-minded attitude to people will always shine in our hearts. We sincerely thank Dr. M. Holmgren for his consistent and instructive help on data collection, data interpretation and writing after Dr. Rakowski passed away. We also thank Dr. J. Duerr and R. DiCaprio for their patient help with writing; Dr. J. D. Horisberger and Dr. O. Capendeguy for providing cDNAs of *Bufo* NKA α_1 and β_1 and the reviewers for their constructive comments. Research was supported by NIH grant NS-022979 to R. F. R.

Appendix: Equations and Reaction Schemes

Reaction happening in electroneutral Na^+/Na^+ exchange mode in the absence of ADP can be expressed as

$$E1P(Na3) \leftrightarrow E2P + 3Na^+. \qquad \text{(Scheme 2)}$$

Under this condition, ideally there are no changes of Q_{tot} with V_h. The charge translocation can be expressed as a Boltzmann distribution:

$$\frac{Q(V) - Q_{min}}{Q_{tot}} = \frac{1}{1 + \exp\left[\frac{zF(V_{mid} - V)}{RT}\right]} \qquad (1)$$

Reaction in the presence of ADP is extended and can be expressed as

$$3Na_i + E_iATP \overset{K_m(V_h)}{\leftrightarrow} (Na_3)E_1P \cdot ADP \underset{\kappa_{-1}}{\overset{k_1}{\rightleftharpoons}} (Na_3)E_1P \underset{\kappa_{-2}}{\overset{k_2}{\rightleftharpoons}} E_2P + 3Na_o \qquad \text{(Scheme 1)}$$

Reaction in the presence of ADP can also be expressed as a detailed form:

$$\begin{aligned} E1 \cdot ATP + 3Na &\leftrightarrow E1 \cdot ATP \cdot 3Na \leftrightarrow E1P(Na_3) \cdot ADP \\ &\leftrightarrow E1P(Na_3) \leftrightarrow E2P \cdot 3Na \leftrightarrow E2P \cdot 2Na \\ &\leftrightarrow E2P \cdot Na \leftrightarrow E2P \end{aligned} \qquad \text{(Scheme 3)}$$

Pumps can exit from the subset of charge translocation transition at any step of Scheme 3. Holmgren and Rakowski (2006) predicted pumps could exit to the left of $E1P(Na_3)$ in Scheme 3, but the manipulation of $[Na^+]_i$ and $[ADP]_i$ in our present study failed to bring pumps to exit in this direction. Unexpectedly, in low $[Na^+]_o$, pumps might exit the subset of charge translocation transition through direct dephosphorylation of E2P to E1.

References

Albers RW (1967) Biochemical aspects of active transport. Annu Rev Biochem 36:727–756

Apell HJ (2003) Structure–function relationship in P-type ATPases—a biophysical approach. Rev Physiol Biochem Pharmacol 150:1–35

Boardman LJ, Lamb JF, McCall D (1972) Uptake of [^{3}H]ouabain and Na pump turnover rates in cells cultured in ouabain. J Physiol 225:619–635

Colina C, Rosenthal JJC, DeGiorgis JA, Srikumar D, Iruku N, Holmgren M (2007) Structural basis of Na^+/K^+-ATPase adaptation to marine environments. Nat Struct Mol Biol 14: 427–431

De Weer P (1970) Effects of intracellular adenosine-5'-diphosphate and orthophosphate on the sensitivity of sodium efflux from squid axon to external sodium and potassium. J Gen Physiol 56: 583–620

Domaszewicz W, Apell H (1999) Binding of the third Na+ ion to the cytoplasmic side of the Na, K-ATPase is electrogenic. FEBS Lett 458:241–246

Garrahan PJ, Glynn IM (1967) The stoichiometry of the sodium pump. J Physiol 192:217–235

Glynn IM, Hoffman JF (1971) Nucleotide requirements for sodium-sodium exchange catalysed by the sodium pump in human red cells. J Physiol 218:239–256

Glynn IM, Karlish SJD (1976) ATP hydrolysis associated with an uncoupled sodium flux through the sodium pump: evidence for allosteric effects of intracellular ATP and extracellular sodium. J Physiol 256:465–496

Heyse S, Wuddel I, Apell HJ, Sturmer W (1994) Partial reactions of the Na, K-ATPase: determination of rate constants. J Gen Physiol 104:197–240

Hilgemann DW (1994) Channel-like function of the Na, K pump probed at microsecond resolution in giant membrane patches. Science 263:1429–1432

Holmgren M, Rakowski RF (1994) Pre-steady-state transient currents mediated by the Na/K pump in internally perfused *Xenopus* oocytes. Biophys J 66:912–922

Holmgren M, Rakowski RF (2006) Charge translocation by the Na^+/K^+ pump under Na^+/Na^+ exchange conditions: intracellular Na1 dependence. Biophys J 90:1607–1616

Holmgren M, Wagg J, Bezanilla F, Rakowski RF, De Weer P, Gadsby DC (2000) Three distinct and sequential steps in the release of sodium ions by the Na^+/K^+-ATPase. Nature 403:898–901

Horisberger J-D, Kharoubi-Hess S (2002) Functional differences between α subunit isoforms of the rat Na, K-ATPase expressed in *Xenopus* oocytes. J Physiol 539:669–680

Kimura J, Miyamae S, Noma A (1987) Identification of sodium calcium exchange current in single ventricular cells of guinea-pig. J Physiol 384:199–222

Nakao M, Gadsby DC (1986) Voltage dependence of Na translocation by the Na/K pump. Nature 323:628–630

Peluffo RD (2004) Effect of ADP on Na+–Na+ exchange reaction kinetics of Na, K-ATPase. Biophys J 87:883–898

Peluffo RD, Arguello JM, Lingrel JB, Berlin JR (2000) Electrogenic sodium–sodium exchange carried out by Na, K-ATPase containing the amino acid substitution Glu779Ala. J Gen Physiol 116:61–73

Post RL, Hegyvary C, Kume S (1972) Activation by adenosine triphosphate in the phosphorylation kinetics of sodium and potassium ion transport adenosine triphosphatase. J Biol Chem 247:6530–6540

Rakowski RF (1993) Charge movement by the Na/K pump in Xenopus oocytes. J Gen Physiol 101:117–144

Rakowski RF, Paxson CL (1988) Voltage dependence of Na/K pump current in Xenopus oocytes. J Membr Biol 106:173–182

Rakowski RF, Gadsby DC, De Weer P (1989) Stoichiometry and voltage dependence of the sodium pump in voltage-clamped, internally dialyzed squid giant axon. J Gen Physiol 93:903–941

Rakowski RF, Vasilets LA, LaTona J, Schwarz W (1991) A negative slope in the current-voltage relationship of the Na^+/K^+ pump in *Xenopus* oocytes produced by reduction of external $[K^+]$. J Membr Biol 121:177–187

Rakowski RF, Gadsby DC, De Weer P (1997) Voltage dependence of the Na/K pump. J Membr Biol 155:105–112

Sagar A, Rakowski RF (1994) Access channel model for the voltage dependence of the forward-running Na^+/K^+ pump. J Gen Physiol 103:869–893

Skou JC, Esmann M (1992) The Na, K-ATPase. J Bioenerg Biomembr 24:249

Taglialatela M, Toro L, Stefani E (1992) Novel voltage clamp to record small, fast currents from ion channels expressed in *Xenopus* oocytes. Biophys J 61:78–82

Wuddel I, Apell HJ (1995) Electrogenicity of the sodium transport pathway in the Na, K-ATPase probed by charge-pulse experiments. Biophys J 69:909–921

Yang XC, Sachs F (1989) Block of stretch-activated ion channels in *Xenopus* oocytes by gadolinium and calcium ions. Science 243:1068–1071